

# Nanomaterials under high-pressure†

Alfonso San-Miguel

Received 9th July 2006

First published as an Advance Article on the web 10th August 2006

DOI: 10.1039/b517779k

The use of high-pressure for the study and elaboration of homogeneous nanostructures is critically reviewed. Size effects, the interaction between nanostructures and guest species or the interaction of the nanosystem with the pressure transmitting medium are emphasized. Phase diagrams and the possibilities opened by the combination of pressure and temperature for the elaboration of new nanomaterials is underlined through the examination of three different systems: nanocrystals, nano-cage materials which include fullerites and group-14 clathrates, and single wall nanotubes. This tutorial review is addressed to scientist seeking an introduction or a panoramic view of the study of nanomaterials under high-pressure.

## 1. Introduction

Nanomaterials are expected to be at the heart of the next technological revolution in solid-state electronics, to emerge as new structural materials, to serve as systems for controlled drug delivery and to have a considerable impact in practically all domains of science. Nanostructure based devices taking advantage of their unique functional properties (chemical, optical, magnetic, mechanical, optoelectronic, *etc.*) are likely to become ubiquitous. It is then not surprising that high-pressure investigations of nanomaterials develop in parallel to the growth of nanosciences either to better understand the properties of nanomaterials or to provide alternative methods for nanostructuration.

Université Lyon 1 and CNRS, Laboratoire de Physique de la Matière Condensée et Nanostructures, UMR 5586, 43 Bvd 11 Novembre 1918, 69622 Villeurbanne, France. E-mail: sanmiguel@lpmcn.univ-lyon1.fr

† The HTML version of this article has been enhanced with colour images.



Alfonso San Miguel

Professor A. San-Miguel is the Group Leader of the Nanomaterials Under Extreme Conditions Section at the "Laboratoire de Physique de la Matière Condensée et Nanostructures" in Lyon 1 University and CNRS, France. After a BS degree in Physics at Barcelona in 1989, Prof. San-Miguel received his PhD in Physics from the University P&M Curie, Paris in 1993. There followed 4 years at the European Synchrotron Radiation before he joined the University Lyon 1 in 1997 as associated professor. He was appointed as full professor in 2003. His research interests cover all aspects of condensed matter under extreme conditions of pressure, from semiconductors to molecular systems, intercalation or nanomaterials.

After a BS degree in Physics at Barcelona in 1989, Prof. San-Miguel received his PhD in Physics from the University P&M Curie, Paris in 1993. There followed 4 years at the European Synchrotron Radiation before he joined the University Lyon 1 in 1997 as associated professor. He was appointed as full professor in 2003. His research interests cover all aspects of condensed matter under extreme conditions of pressure, from semiconductors to molecular systems, intercalation or nanomaterials.

The existence of a characteristic length scale less than  $\sim 100$  nm is the mark of nanomaterials. This length scale can be for instance a particle diameter, grain size, layer thickness, tube diameter or length. The routes for the synthesis of materials exhibiting such type of length scales are as varied as the imagination of scientists and include membrane-template methods, mechanical attrition, sol-gel process, chemical vapour deposition, flame or arc-discharge methods, *etc.* The results are systems which dimensionally can be considered as zero, one or two depending on the number of nano-length Cartesian scales associated with the object. Nanostructuration is not by far confined to human imagination and is also an important choice of Nature, for instance in clays, circumstellar dusts or many biological systems.

Interactions at the nanoscale are usually governed by the fact that the characteristic nanolength becomes comparable with other critical lengths of the system as mean free-paths, scattering or coherence lengths. At the same time, confinement translates in a reorganization of the electronic density of states towards more discretized states (Fig. 1). These two consequences of nanostructuration and their combinations lead to the so-called quantum related effects which determine most of the characteristic properties of nanomaterials. A major consequence of nanoconfinement is the elevated ratio of the number of surface to volume atoms, which becomes another key point for the understanding of nanomaterials properties. The ratio of the number of surface to the total number of atoms, goes from  $10^{-20}$  or less in bulk materials to values close

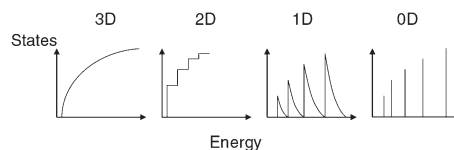


**Fig. 1** Scheme of the evolution of the electronic density of states (e-DOS) with nanostructuration. From left to right is shown the progression of the e-DOS from a 3-dimensional solid. The reduction of one of the Cartesian dimensions up to nanometric dimensions leads to a 2-D solid, reduction of two of the Cartesian dimensions gives a 1-D solid and the reduction of all 3 Cartesian dimensions generates a 0-D solid.

to unity in small nanoclusters, for which it scales as  $\sim 1/(\text{Particle diameter})^3$ , and exactly one in nanotubes or fullerenes. Nano-objects can be viewed as intermediate systems between single atoms or molecules and bulk matter. Physical and chemical properties of nanomaterials can then be in general totally different from their bulk counterparts, strongly dependent on size and offering new paths for chemistry developments.

An additional feature of many nanomaterials that can also play a role in high-pressure studies is porosity. This can be an intrinsic feature as for fullerenes or nanotubes or it can be related or reinforced by the assemblage of nanomaterials as in bundles of nanotubes, fullerites or in assemblages of nanoparticles. Fig. 2 illustrates these ideas in the case of a number of carbon nanostructures. Porosity increases the potential for intercalation and then the elaboration of new nano-systems. As we will also discuss later, a low compacity is also an open door for complex interactions between the system and the pressure transmitting medium.

What are the expected effects or benefits of very high-pressures on nanomaterials? In the case of homogeneous systems, *i.e.*, excluding heterostructures or nanocomposites, the ultimate effect of pressure will be the destruction of nanostructure. For instance, carbon nanotubes at extremely high-pressures will be probably transformed into a single crystal diamond or a graphite powder, but as we will later discuss, before this transformation can take place, many other different nanostructures can be obtained including nano-diamond or nanotube polymers. A first benefit of high-pressure is then the potential for obtaining new phases, of nanostructure nature too. In fact, the volume reduction induced by pressure is an immediate route for increasing the interaction among nano-objects or between host nanostructures and guest atoms/molecules, or inside the nanostructure

itself. This eventually leads to chemical reactions or phase transformations. We can then distinguish at least three types of pressure induced modifications:

a) Transformation of the nano-constitutive elements. This can be for instance a structural modification in a nanoparticle, the collapse of a nanotube or the destruction of a fullerene.

b) Transformation of the interaction between nano-objects. We can see here the polymerization of nanotubes or fullerenes or the assemblage between nanoparticles. In fact, pressure induced assembling, applies to all systems from the simplest molecule (hydrogen).

c) Modification of interactions between the nano-object and the pressure transmitting medium.

As in any chemical process, the simultaneous application of temperature is a crucial step either to overcome reactive barriers or to introduce the rotational energy needed for a correct assemblage of nano-constituents. High-pressure and high-temperature application have the potential for the exploration of an infinity of paths for nano-assembling or phase transformation in a controlled way and constitutes a unique route for the elaboration of new materials. Pressure application, as for bulk materials, allows the continuous modification of the interatomic interactions inside the nano-object or between nano-objects and constitutes an invaluable tool to explore physico-chemical interactions at the nanoscale and their link with physical properties of interest.

Pressure application implies the use of a pressure transmitting medium (PTM) or alternatively the use of the compressed system itself as pressure transmitting medium. In the case of nanomaterials, the relevance of the surface atoms places the interaction with the PTM in a first plane. The parameters determining the importance of such interactions comprise a) the chemical reactivity of the nanoparticle which depends on the degree of surface passivation, b) the reactivity of the PTM

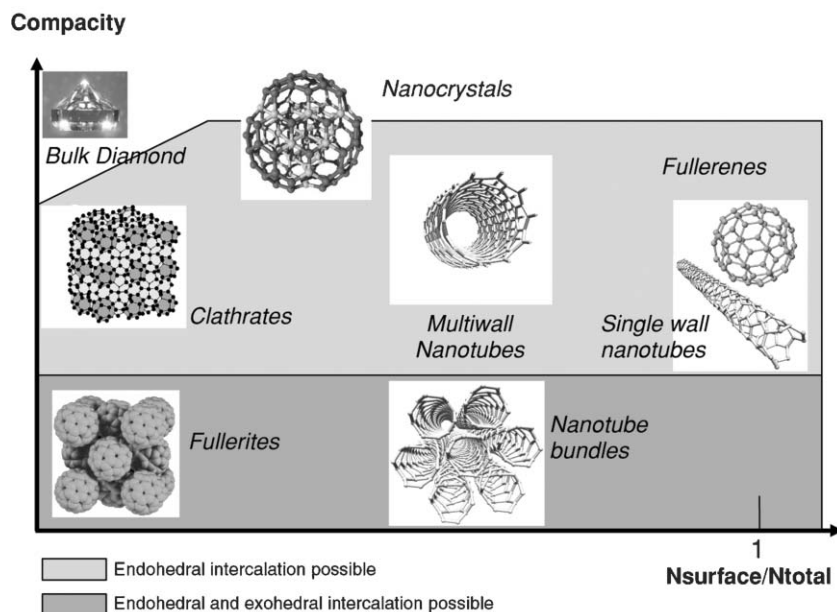


**Fig. 2** Sketch of main carbon existing and potential (clathrate) nanostructures in a space of compacity *versus* the ratio of surface atoms to the total number of atoms of the structure. Diamond has also been included for comparison. Proximity towards the lower right corner indicates the potential of the nanostructure for interaction with a pressure transmitting medium either chemically or through intercalation.

with the surface atoms of the nanomaterials, c) the potential intercalation of the PTM in the nanosystem. The system porosity opens new channels for reinforced interactions with the PTM. In particular forms of intercalation or nano-confined structuration of the PTM can appear. The compression of highly porous nanomaterials having important atomic surface ratios can become the compression of a new system made of the nanomaterials + PTM.

The aim of this tutorial review is to show how extreme conditions of pressure contribute to the synthesis of new nanomaterials and how pressure can be used to study the effect of structuration or confinement at the nanometer scale. We will discuss the use of pressure in the synthesis and study of properties of “pure” nanosystems in contrast to “composed” nano-systems as nano-layers or nano-composites. This restriction is mainly related to the author’s research activities and does not mean that high-pressure investigations of these composite systems are not important. For instance, superhard nanocrystallites embedded in a strong amorphous matrix is currently one of the most promising concepts for the synthesis of novel superhard materials.

We will consider three groups of nanomaterials and study separately the contribution of pressure to the chemistry of these materials.

First of all we will speak about nanoparticles which in principle correspond to the simpler idea of nanostructuration, *i.e.*, the sole reduction of size with respect to the bulk in the three Cartesian coordinates. The high-pressure behaviour of the obtained nanoclusters or nanocrystallites can differ remarkably with respect to the bulk and their study is not only of fundamental importance, but also offers routes for the elaboration of new nanomaterials whose properties can be tuned with the nanoparticle size. Their understanding is also important in regard to nano-composite systems for which they are the elemental constituents. They are also the closest idea to the ideal case of 0-D systems in Fig. 1 and to high compact nanostructures which simplifies the interaction with the pressure transmitting medium, if the surface has been passivated (Fig. 2).

The second family of materials to be considered has been grouped in the term nano-cage materials. The essence of such systems is the existence of cavities of nanometer size. The type of assemblage existing between the nano-cage will determine two different cases: fullerites, which are assemblages of fullerenes exhibiting interactions that range between weak van der Waals forces up to covalent ones; and group 14 clathrates made of small cages of 20 to 28 atoms assembled in compact crystalline face-sharing arrangements. As we will see, the clathrate forms here considered can also be classified as zeolites. We will only consider the case of well organised nano-cages and avoid the discussion of nano-porous systems.

Nanotubes will constitute the last case to be discussed. Their particular nanostructuration leads to self-sustained and almost ideal 1-D structures (Fig. 1). Their simplicity is only apparent. As shown in Fig. 2 they allow for the lowest structural compacity and hence the highest interaction with the pressure transmitting medium and the highest intercalation capabilities. We will centre the discussion on studies of single wall carbon nanotubes, which are by far the most studied systems.

The order chosen to introduce these three families of materials is related to their situation on the plot in Fig. 2. We have chosen to present first systems whose interaction with the pressure transmitting medium is lower (upper left corner) and continue from there to the systems at the right lower corner having then the maximum interaction with the PTM. This introduces a progression on the complexity of the system. We will try to introduce general results whenever it is possible and to illustrate them through the best documented examples.

## 2. Nanoparticles or nanoclusters (nanocrystallites, nano-amorphous)

Nanoparticles are aggregates of atoms or molecules of nanometric size, containing a number of constituent particles ranging from  $\sim 10$  to  $10^6$ . Under the general term nanocluster or nanoparticles, some distinctions are possible as nanocrystals or nanoamorphous. The study of nanoparticles under high-pressure is considered as a possible path to expand the range of available solid-state materials. High-pressure methods allow for the synthesis of new materials through the metastabilization of the high-pressure phases after  $P$ – $T$  cycle. Synthesis of diamond from graphite is the best known case. But, many pressure induced transformations are reversible, meaning that the window opened by high-pressure to the synthesis of new polytypes, closes on pressure release. We will see that the properties of nanocrystals lead to the possibility not only of leaving this window wide open, but also of changing the landscape that we can see through it.

From all possible nanocrystals systems, most high-pressure studies involve covalent bonded materials (simple semiconductors, oxides). The main reason is that a stronger inter-atomic interaction will enhance nano-size effects. This is easy to understand from a view of Fig. 1. A very weak interaction, van der Waals for instance, will lead to weak modification of the atomic electronic states. Then the condensed system finds itself with an electronic density of states close to the 0-D case of Fig. 1 independently of the size of the particle, a situation that is totally opposite for a strong interacting system. In addition, the elaboration and manipulation of sufficiently large quantities of material for high-pressure studies, is facilitated in strong covalent materials. We will then concentrate our discussion on covalent nanocrystals and try to bring through the best documented examples the main ideas on the chemistry that can develop through nanocrystal pressurization.

Before going into examples, let us consider some of the general ideas that emerge from the high-pressure investigation of nanocrystals. In a solid–solid phase transformation accompanied by a change of volume, single crystals fragment in domains of nano- or micrometer size by processes that include twinning or fracture. This phenomenon is exploited for instance for the synthesis of steels with improved mechanical properties, but complicates the study of the atomic paths in displacive phase transformations. Nanocrystals can be smaller than these fragment domains allowing for the existence of a critical nanocrystal size<sup>1</sup> that, in principle, enables the study of crystallites without interior crystalline defects or fracturing<sup>2,3</sup> (Fig. 3). Nanocrystals are often externally faceted showing a defined shape which is directly related to its crystallographic

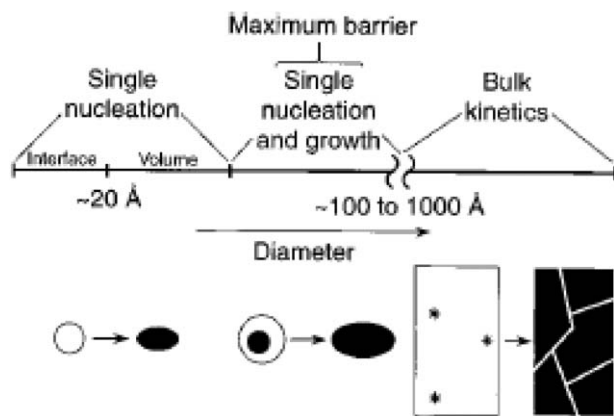


**Fig. 3** Illustration of the various size regimes of the kinetics of solid–solid phase transitions. Defects, which act as nucleation sites, are indicated by asterisks in the cartoon of the bulk solid. (Reproduced with permission from Ref. 2. Copyright 1997, AAAS.)

structure. Phase transitions can involve or not a modification of shape, but in all cases the surface energy associated plays an important role on the phase transformation dynamics. Another point of view is that the number of surface atoms in a nanocrystal can become dramatically important and show significant surface reconstructions and energies. For very small clusters, the involved energies can be so high that the high-pressure phase of the structure is found at ambient conditions in the synthesized nanocrystal. This has been in fact reported for instance in 2 nm CdS nanocrystals<sup>4</sup> whose structure tends towards the 6-fold coordinated rocksalt structure, *i.e.*, the first high-pressure polytype.

These differences from the bulk determine a different phase diagram of nanocrystallites as a function of pressure and temperature, opening the door to the metastabilization of new crystalline forms at ambient pressures which can allow exploiting different physical properties for applications. The term “metastability” is used here to refer to a phase differing from the bulk stable phase at the same thermodynamic conditions. We could also have chosen to speak about size dependent equilibrium stability. The surface to volume ratio and the probability of monodomain crystallites evolve inversely with the size of the nanocrystallite. This has, as a consequence, nanocrystallite size dependent thermodynamics and kinetics of phase transformations. The study of nanosize induced metastability—with respect to the bulk phase diagram—as a function of the size of the crystal has been considered as analogous to supercooling in liquid droplets, due to the confinement or to magnetic transitions as the size of the particle allows the modulation of crystalline domains. Nevertheless the intrinsic difference between these phenomena rapidly imposes limits to these analogies. The single nucleation characteristic phase transition of small nanocrystals allows the investigation of the mechanism of first order phase transformations. Understanding of the metastability of different bonding schemes can be made clearer through the investigation of the microscopic mechanisms by which solids transform between crystal structures. In particular the nanocrystal shape changes at the phase transition are constrained by the microscopic mechanism of the displacive phase transition.

Even if all these factors contribute to make the experimental panorama a bit confusing, the work of the many groups from which we can underline the contribution of the Alivisatos group at the University of California, start to render a clear and simple image of some general trends of the properties of nanocrystals under high-pressure. Simple energetic considerations lead to distinguish three main factors determining the sign and amplitude of the difference of transition pressure between the bulk and the nanoparticle:<sup>5,6</sup> a) the difference of surface energy of the involved phases; b) the difference of internal energy of the two bulk phases; c) the volume change of the bulk and the nanoparticle at the transition. Nevertheless, this simple image of single structured nanocrystal is not supported by all studies and, for instance, some detailed X-ray diffraction studies tend to sustain the idea of nanocrystals composed of a core and shell with differentiated structures.<sup>7</sup> This is also supported by *ab initio* calculations in small carbon nanoclusters.<sup>8</sup>

In principle, a different combination of the above energy contributions could give rise to transition pressures with values higher, lower or equivalent to the ones of the bulk material. In fact, all different cases have been reported in various systems. Nevertheless, one needs to be extremely careful to integrate the different experimental factors affecting the study. A remarkable case is the  $\gamma$ -Fe<sub>2</sub>O<sub>3</sub> (maghemite) to  $\alpha$ -Fe<sub>2</sub>O<sub>3</sub> (hematite) transition pressure which in several works has been reported to increase with an increase in size of the nanocrystals. Very recently, a more detailed work<sup>9</sup> points to totally reverse conclusions: the transition pressure decreases with the increasing size of the nanoparticle and saturates at a particle size of roughly 7 nm, from which the bulk transition pressure is observed. This is the same type of result that has been more usually observed, in particular in systems like semiconductors of the group IV or III–V or II–VI. The surface energy term is dominant, and the stability under high-pressure or under high-temperature of nanocrystals is essentially related to it. In fact, it is easy to understand why with a decreasing size of the nanocrystal in these system one observes that:<sup>10</sup> i) the melting point decreases, ii) the pressure induced solid–solid phase transition takes place at higher pressures, iii) the reverse solid–solid phase transition takes place with a larger hysteresis than in the bulk. In fact, cluster surface atoms tend to be coordinated unsaturated, giving rise to a large surface energy which is always higher than in the liquid phase. On the other side, in solid–solid phase transformation, the symmetry of the involved phases dictates the lower energy shape of the nanocrystal. Depending on the pathway of the transformation, more or less disordered high-energy surfaces will be generated, causing a delay in the solid–solid transformations.

The general trend is then that more energy, and hence more pressure is needed to induce solid–solid transitions transformation in nanocrystals. Larger hysteresis, *i.e.*, differences between the upstroke and downstroke transition pressures are generally observed for nanocrystals. One can then expect that for a critical nanocrystal size domain, the high-pressure phase could be metastabilized. The many factors influencing the energetics or kinetics of such processes lead to a variety of behaviour.

Let us now consider a few of the best studied examples which illustrate the interest of high-pressure investigation of nanocrystals, in particular for the elaboration of new polytypes whose properties can be totally different from the stable phase at ambient conditions. The CdSe nanocrystal system has been used as a model for structural studies. The nanocrystals undergo the same structural transition as in corresponding bulk, *i.e.* from the 4-fold coordinated hexagonal wurtzite structure to the 6-fold coordinated cubic rocksalt one with an 18% reduction in volume. This transition takes place in the bulk between 2 and 3 GPa in the upstroke process with an hysteresis of approximately 1 to 2 GPa. Nanocrystals can be obtained nearly monodisperse and as nearly defect-free crystals with controlled shape. Such nanocrystals can reversibly transform back and forth between both phases as a single domain without fracture or twinning for particle sizes up to 13 nm. The transformation proceeds through a local nucleation and growth mechanism arising from a shearing motion of the crystal, with a critical nucleus size comprised of several atomic planes (see Fig. 4). In the case of CdSe nanocrystals, the upstroke transition pressure shifts towards higher pressures when reducing the size of the nanocrystal (Fig. 5), and the hysteresis loop width attains a value 6 GPa independently of the nanocrystal size and displays simple transition kinetics as compared with the extended solid.<sup>11</sup> This leads to the existence of a critical size domain for the stabilization of the rocksalt high-pressure phase at ambient pressure starting from  $\sim 11$  nm and extending towards higher sizes up to a not yet determined critical value. There exist cases where complete trapping of the high pressure phase needs the modification of temperature. This is for instance the case of ZnO which as CdTe crystallizes in the hexagonal wurtzite structure and transforms under high-pressure into the cubic NaCl-type structure but at a higher pressure of 9 GPa. Total trapping of the cubic ZnO phase was only obtained by the heat treatment at high-pressure (15 GPa and 550 K) of the w-ZnO nanocrystallites.<sup>12</sup>

Amorphous phases can also be generated through the high-pressure treatment of nanocrystals. The kinetic trapping of

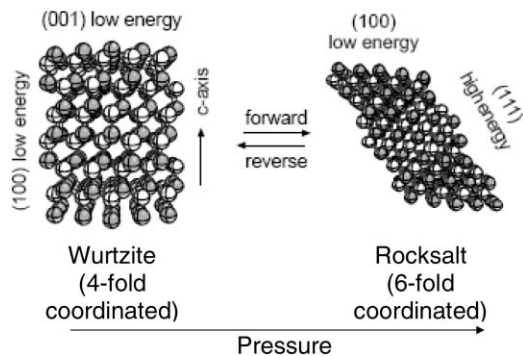


**Fig. 4** Scheme showing the shape change in CdSe nanocrystals at the phase transformation from wurtzite and rocksalt structures. The shape change exposes high-energy rocksalt faces, such as the (111) face, that would otherwise not be exposed in an annealed particle. The shape change takes place because the transition is a single-domain process and room temperature is too low for surface rearrangement to occur, as it is below the 575 K limit at which interparticle diffusion occurs and the crystals begin to aggregate. (Reproduced with permission from Ref. 44. Copyright 2002, American Chemical Society.)

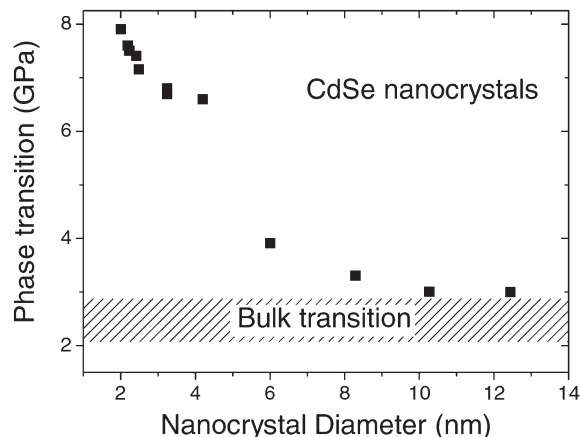


**Fig. 5** Phase transition of wurtzite CdSe nanocrystals towards rocksalt structure as a function of the diameter of the crystal. (Adapted from Refs. 5 and 11.) The phase transition is taken at the midpoint of the hysteresis loop.

amorphous Si nanoclusters upon release of pressure from the high-pressure form of silicon (the  $\beta$ -Sn phase) was obtained by S. H. Tolbert *et al.*<sup>13</sup> This behaviour differs from bulk silicon, which following the same thermodynamic path transforms commonly to a slightly distorted tetrahedral phase known as BC8. In this experiment, nanocrystals with sizes between 10 and 50 nm passivated by a thick 1.5 nm layer of SiO<sub>2</sub> were synthesized by gas pyrolysis of Si<sub>2</sub>H<sub>6</sub> and O<sub>2</sub> and then pressurized with ethylene glycol as pressure transmitting medium. Amorphization was also observed in silicon upon compression on films of porous Si, which contains nanometre-sized domains of diamond-structured material. A pressure induced amorphization at pressures above 10 GPa<sup>14</sup> was observed. The high density amorphous phase was shown to transform to low-density amorphous silicon upon decompression.

Size-selectivity in nanocrystals can concern more than two competing phases and this is well illustrated in the case of TiO<sub>2</sub> anatase nanocrystals, which exhibit a strong size-dependent phase selectivity at high-pressures (Fig. 6), with the observation of amorphous, baddeleyite or  $\alpha$ -PbO<sub>2</sub> (as bulk anatase) structures with increasing size of the nanoparticles [Ref. 15 and references therein]. As for silicon, TiO<sub>2</sub> amorphized nanoparticles exhibited a high to low density amorphous polymorphism under pressure release.

As we have noted, the surface energy balance often gives rise to pressure induced shape changes of nanocrystallites. Of course the initial shape of the crystal will then play a key role on the transformation and its final shape has the potential to inform us on the atomic kinetics associated with a given structural transformation. Nanocrystal shape changes were first evidenced in 1994 in crystalline silicon.<sup>13</sup> Some years later (see Fig. 4), we should underline the investigation through pressure cycling of the wurtzite to the rocksalt transition of CdSe allowing to propose a mechanism of sliding planes to relate both structures.

All these examples serve to illustrate the potential of high-pressure for the understanding of fundamental phenomena and for the elaboration of new nanocluster materials starting from existing ones. The combination of high-pressure with high-temperature allows extending the possibilities for new

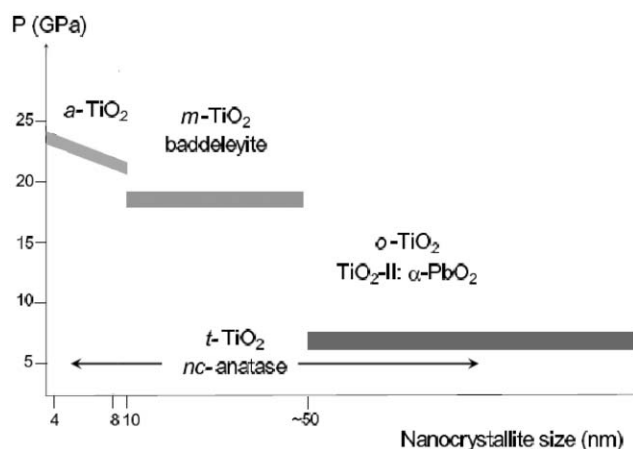


**Fig. 6** Size-dependent pressure stability diagram of nanocrystalline tetragonal anatase (*t*-TiO<sub>2</sub>). Nanocrystals of size <10 nm undergo pressure induced amorphization and remain amorphous (*a*-TiO<sub>2</sub>) upon further compression and decompression. Approximately 12–50 nm crystallites transform to monoclinic baddeleyite structured TiO<sub>2</sub> (*m*-TiO<sub>2</sub>) upon compression, which then transforms to  $\alpha$ -PbO<sub>2</sub> structure (*o*-TiO<sub>2</sub>) on decompression. Coarser crystallites transform directly to *o*-TiO<sub>2</sub>. (Reproduced with permission from Ref. 15. Copyright 2006, American Physical Society.)

nanostructuration as we have seen for the case of ZnO, and its exploration is just starting. The metastabilization of high pressure or amorphous phases *via* pressure application on nanocrystals can be combined with the introduction of fluorescence centers or magnetic atoms for instance in view of applications.

Finally we can note that one of the strategies in the search for superhard materials has been the fabrication and characterization of new forms of diamond. Nanocrystalline diamond occupies a central part as its mechanical properties appear to be superior to those of single crystalline diamond. In particular the elaboration of nanodiamond from bulk graphite through combined high-pressure and high-temperature application appears very promising.<sup>16</sup> The structure of nanodiamond is predicted to be size-dependent and small nanodiamond crystals of the order of  $\sim 2$  nm could be intermediate between fullerenes and diamond crystals, namely made of a core of diamond with several half caps of fullerenes (see the nanocrystal of Fig. 2 from Ref. 17). This type of structure if confirmed, allows new paths for carbon doping, through endohedral intercalation in the half fullerenes. As we will discuss later, nanodiamond can also be obtained from fullerenes or nanotubes.

### 3. Nano-cage materials: clathrates and fullerites

Fullerites and group 14 clathrates are both solid state assemblages of covalent nano-cages made of at least 20 atoms.

**Table 1** Structural and bond characteristics of fullerites and clathrates

	Fullerites	Group 14 Clathrates
Cage bonding	sp <sup>2</sup> type	sp <sup>3</sup> type
Inter-cage bonding	van der Waals or sp <sup>3</sup> cage-linkage through cycloaddition	sp <sup>3</sup> type through face sharing
Number of cage atoms	From 20 to “∞”, but mainly 60 and 70	20 + (24 or 28)
Intercalation type	Endohedral or Exohedral	Endohedral
Known/hypothetical cages	C/BN	Si, Ge, Sn/C

As shown in Fig. 2, both systems are extended solids and nanostructuration is due to the presence of nano-cages. Fullerites and clathrates are conceptually close structures but their chemistry is totally different and it has evolved from totally different concepts. Nevertheless, as we will discuss later, high pressure leads to a convergence of the two systems through the development of sp<sup>3</sup> linkage between fullerenes. In Table 1 are summarized the main differences and similarities between the two families of nano-cage materials that will be further developed in the next sections.

In the case of fullerites, even if some work has been done on C<sub>70</sub> fullerites, the broader part of the literature concentrates on the C<sub>60</sub> case. We will confine our discussion to this case.

#### 3.1. Fullerites

The development of the chemistry of fullerenes was started in the mid 80's by Smalley and co-workers at Rice University. Fullerites are associations of fullerene atoms. The best known and studied fullerites are those made of C<sub>60</sub> units. At ambient conditions C<sub>60</sub> crystallizes in an fcc structure (see Fig. 2) characterized by the van der Waals assemblage of the nano-cages. Inter-cage covalent bonds can be obtained by different means including visible or UV light exposure, doping and through high-pressure treatment. Several reviews have appeared on the high-pressure and high-temperature properties of C<sub>60</sub> fullerites and we refer the reader to recent ones<sup>18,19</sup> and references therein for more details. The existing literature on the study of fullerene under high pressure conditions includes now an important number of works that will be difficult to cover extensively in this tutorial review. So we will restrict ourselves mainly to discuss pressure induced polymerization phenomena as it constitutes a route for the elaboration of new carbon forms with improved properties. The existence of high-pressure superhard phases and the not yet well explained observed magnetism of some polymer phases, comprise an important part of present investigation efforts.

The relative ease with which C<sub>60</sub> fullerenes assemble, can be understood as due to the presence of pentagonal rings, having as consequence that the C<sub>60</sub> behaves as an unsaturated organic molecule with 30 reactive double bonds. At ambient conditions the C<sub>60</sub> molecules crystallize in the fcc structure, with the molecules rotating freely. After compressions at high-pressure above 2 GPa the molecules tend to freeze in a rotational glass. The key factor in optimizing the long range order of high-pressure polymerized solids will then be to keep the spheroids rotating as freely as possible by increasing the synthesis temperature. The system will, in this way, more completely homogenize the number of bonds per molecule and ordered phases will thus be stabilized. Some precautions need to be taken on compression studies of fullerites. As we have shown

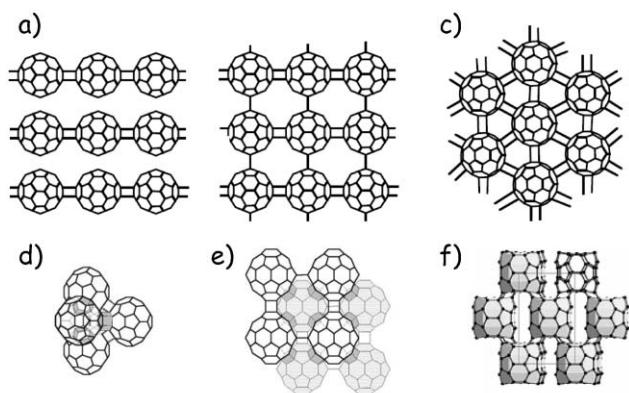


**Fig. 7** Schematic structural arrangement of  $C_{60}$  molecules in different phases. Top Row, from left to right: three experimentally observed polymerized fullerite structures all issued from 2 + 2 cycloaddition bonding: (a) orthorhombic structure where each molecule is bonded to the two nearest neighbours along a  $\langle 110 \rangle$  fcc direction forming parallel chains; (b) “tetragonal” lattice where each molecule is bonded to its four nearest neighbours in a (100) fcc plane and (c) rhombohedral structure where each molecule is bonded to its six neighbours in a high density (111) fcc plane. Second row (d to f): 3-D polymerized structures. (d) elemental 3-D unit derived from the tetragonal structure of b) with an AB stacking and (e) derived from the rhombohedral structure of c) with a ABC stacking. (f) Recently obtained 3-D polymerized structure with 3 + 3 cycloaddition generating  $C_{60}$  8-fold coordinated cuboids. (a to e adapted from Ref. 43; f from Ref. 22.)

in Fig. 2, fullerites offer privileged conditions for nanointercalation, which can consequently modify the initial material. In fact, it has been demonstrated that He,  $O_2$  or  $N_2$  atoms can be easily intercalated in  $C_{60}$  fullerites giving rise to important modification of their properties. Also other pressure transmitting media such as pentane have been shown to react at moderate pressures and temperatures.

The extreme compression of the fcc fullerite can cause the collapse of the fullerene cage and its transformation into other forms of carbon such as polycrystalline cubic diamond, diamond-like materials or graphitic forms. More moderate pressures ( $<15$  GPa) and temperatures ( $<1000$  K) allow the formation of new fullerite phases by chemical bonding between molecules. A very large number of polymerized structures are indeed possible considering the symmetry of the  $C_{60}$  molecule, that of the fcc parent lattice and different types of polymerization reactions. They range from chain-like 1-D polymers to 3-D “clathrate-like” materials. The general trend observed is that the number of bonds between carbon atoms increases with increasing high-pressure and high-temperature conditions (Fig. 7). The known limit is the diamond structure with 4 bonds per atom. In short, between the van der Waals fullerites and diamond, the  $C_{60}$  phase diagram offers a number of different phases that can be characterised as 1-D, 2-D or 3-D polymers with different symmetries.

There have been numerous investigations of the phase diagram of  $C_{60}$ , leading to different propositions with notable differences from one to another. The monomer/polymer  $P$ - $T$   $C_{60}$  equilibrium phase diagram has been investigated in detail in Ref. 20 for pressures below 2 GPa. In the higher pressure domain, we show in Fig. 8 two proposed phase diagram. We should note that  $C_{60}$  not being the stable form of carbon, its “phase diagram” does not correspond with the carbon “equilibrium phase diagram”. The observed differences in published phase diagrams can be attributed to different factors. First we note that some of the proposed phase diagrams were obtained by the *ex situ* investigation of recovered samples after a  $P$ - $T$  cycle (Fig. 8A). The phase diagrams obtained through this procedure should be considered as a “ $P$ - $T$  reactivity diagram” and show the different phases that can be synthesized through quenching procedures. As we have discussed, fullerites favour intercalation and are relative highly reactive. One consequence of this is that most

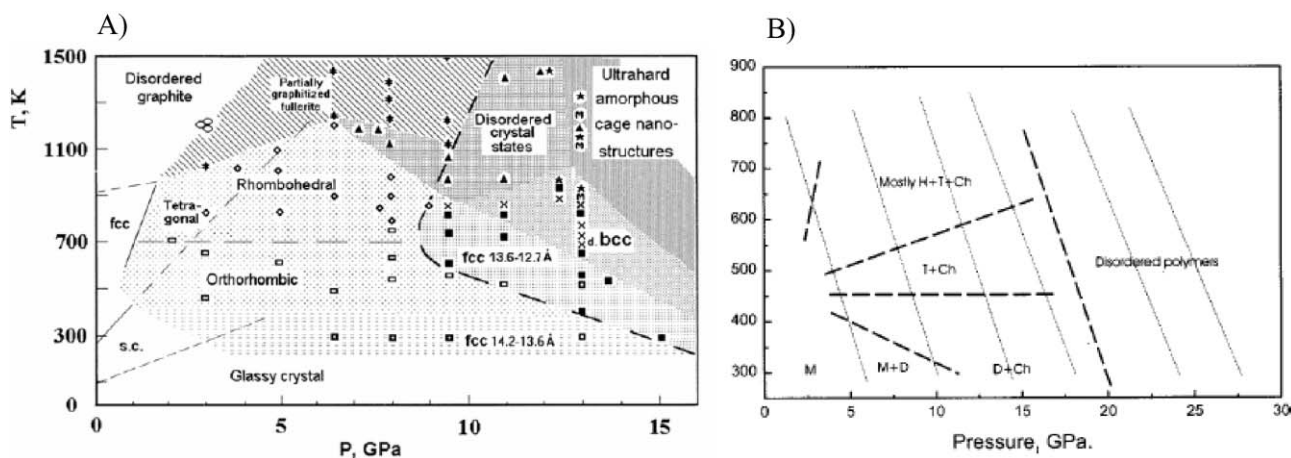


**Fig. 8** Two different Pressure-Temperature diagrams of  $C_{60}$  fullerites underlying different aspects of the  $P$ - $T$  phase diagram. A) Hybrid diagram [Reproduced with permission from V. D. Blank, S. G. Buga, G. A. Dubitsky, N. R. Serebryanaya, N. Yu. Popov and B. Sundqvist, *Carbon*, 1998, 36, 319.<sup>41</sup> Copyright 1998 Elsevier.] The low temperature part (involving fcc, cubic and glassy phase) corresponds to reversible transformation. The high-temperature zone is a “reaction map” of  $C_{60}$  under high-pressure and high-temperature, based mainly on the structure of the recovered samples. B) Phase diagram which underlines the importance of oligomerization and the competition between different polymer phases. M: monomers; D: dimmers; Ch: chain or 1-D polymer; T: tetrapolymer (2-D); H: hexapolymer (2-D). [Reproduced with permission from Ref. 42. Copyright 2002, American Institute of Physics.]

high-pressure studies of fullerites are done without a pressure transmitting medium. Non hydrostatic components which are dependent on the geometry of the pressure application devices, give rise to important deviations from different experiments. In particular, strongly anisotropic compression favours the formation of super-hard phases. Finally, the importance of the dynamics of the fullerenes in the polymerization process, will introduce kinetic factors in the phase transformations which have not been explored in detail. In the following paragraphs we succinctly describe the main facts concerning the high-pressure elaboration of  $C_{60}$  polymers (Fig. 7).

Polymerization between fullerenes takes place *via* the mechanism of cycloaddition. (2 + 2) cycloaddition is at the base of 1-D and 2-D polymers. In the (2 + 2) cycloaddition reaction, a pair of hexagon-hexagon “double bonds,” facing each other in adjacent fullerenes transforms to a single bond, and leads to the formation of two new “single bonds” connecting the fullerenes. Other mechanisms such as (3 + 3) cycloaddition or single cycloaddition are also possible.

Roughly the 1-D polymer structures are found for pressures below 8 GPa and temperatures between ambient and 600–700 K. Polymerization takes place following the shortest (110) direction of the fcc lattice or any of its 12 equivalent directions by (2 + 2) cycloaddition. This multiplicity of choice gives rise to disordered 1-D polymers. Such disorder effects can be reduced either by single crystal work or by introducing a privileged direction through uniaxial pressure application. Partial polymerizations as dimerization or higher order oligomerization have been also observed.

2-D layered polymers of  $C_{60}$  are obtained above approximately 700 K and 1 GPa. Different structures have been determined depending on the final thermodynamic conditions and path followed to reach them, the hydrostatic conditions or the nature of the starting sample (powder or single crystal). Two main classes of structures have been clearly identified. A tetra-coordinated tetragonal (or quasi-tetragonal) class obtained at low pressures and a hexa-coordinated rhombohedral symmetry class mainly at pressures above 6 GPa. Depending on the experimental factors mentioned above, phase mixtures including also the presence of oligomers are observed. The formation of oligomers seems to have a key role in the crystallization process.

Up to now all 3-D  $C_{60}$  obtained polymers exhibit strong structural disorder. The main reason is believed to be the extreme pressure induced reactivity in multiple equivalent directions, related to the proximity of the molecules. As a consequence few detailed structural characterizations exist. Under axial compression without pressure transmitting medium, 3-D  $C_{60}$  polymers which can also be viewed as carbon clathrates or zeolites have been obtained at 12 GPa and 500 K. In this structure, intermolecular bonds exist among all the 12 first neighbours of a pseudo-face centered-cubic fcc  $C_{60}$  network. This phase is characterised by an unusual giant anisotropic deformation, the signature of nonhydrostatic stress present during the synthesis process. This anisotropy related to a larger compression of the crystallographic lattice parameters in the macroscopic direction of compression, is evidenced by the observation of Debye–Sherrer ellipses instead of circular diffraction rings.<sup>21</sup>

Another path for the elaboration of 3-D  $C_{60}$  polymers is the HP-HT treatment of pre-synthesised lower polymer phases. Yamanaka *et al.* applied this procedure for the elaboration of 3-D polymers from a 2-D  $C_{60}$  polymer single crystals at 15 GPa and 900 K.<sup>22</sup> The obtained phases showed a strong deformation of the originally spherical  $C_{60}$  molecule towards a cuboidal shape (Fig. 7c). The  $C_{60}$  cuboids were 8-fold coordinated through [3 + 3] cycloaddition. An important feature of the obtained phase was that it exhibited metallic conductivity; a fact that can most probably be attributed to the presence of disorder. It is also noticeable that the laser-driven shock wave loading of a graphite-copper mixture to about  $14 \pm 2$  GPa and  $1000 \pm 200$  K has been also recently found as a new method for the synthesis of 3-D-polymerized fullerenes.<sup>23</sup> Fullerene interlinking strongly modifies the properties of the different fullerites crystals. As an example, the fcc van der Waals  $C_{60}$  crystal has a bulk modulus of 10–18 GPa and a pressure stability limited to about  $20 \pm 5$  GPa at room temperature, collapsing then into diamond or amorphous  $sp^3$  material. Contrarily a very high bulk modulus of 288 GPa has been measured for 3-D polymerized fullerenes that remain stable at least up to 35 GPa.

Intercalation of  $C_{60}$  with alkali metals can in some cases give rise to the formation of dimers or  $C_{60}$  chains and even 2-D polymers. Until recently high-pressure studies of alkali or alkali earth doped fullerenes concerned mainly superconductivity. In fact, these systems were found to exhibit superconductivity at ambient pressure with maximum values over 30 K. High-pressure studies contributed to elucidate that a high value of the superconducting  $T_c$  was linked to a large lattice volume and consequently that superconducting electron-phonon coupling made intervening normal vibration modes of the fullerene. Recent works have shown that alkali intercalation multiplies at least by a factor of two or three the pressure stability of the original fullerites structure.

Another important phenomena observed in compressed polymeric- $C_{60}$  fullerene is the presence of ferromagnetic interactions with Curie temperatures in the 500–800 K range. The origin of this experimental observation that has been confirmed by various groups is still debated. The magnetic phase appears to be a minority phase distributed within the nonmagnetic matrix formed by the rest of the solid and obtained by pressing and heating up to around 1000 K the rhombohedral or the tetragonal phases of polymeric- $C_{60}$  fullerite. The presence of different fullerene open-cage forms and the formation of vacancies or intercage bond-breaking processes are among the different mechanisms proposed to explain the presence of ferromagnetism in high pressure and high temperature treated fullerenes.

3-D polymerization of intercalation fullerenes will lead to systems that will approach in many senses the known group-14 clathrates that we will describe next. In particular, 3-D polymerization can generate low size fullerene-like cages comparable with those of clathrate structures and with the potential capacity of encapsulating the intercalation atoms. Enhanced superconductivity or “metallic diamond” like properties are among the expected benefits of such, for the moment, hypothetical systems.



### 3.2. Clathrates

The known group-14 clathrates can be considered as 3-D fully polymerized fullerites based on small nanocages of 20, 24 or 28 atoms (Fig. 9). From the different clathrate families, the type-I and type-II structures are of particular interest as the nanocage assemblage totally fills the space with no other voids other than the inner part of the cages. These two clathrate structures are also encountered in clathrate hydrates and correspond respectively to the so called MEP and MTN zeolites topologies which are equally isostructural with the clathrasils (clathrates made of a  $\text{SiO}_2$  framework) structures of melanophlogite and Dodecasil 3C. Both clathrates types are based on the  $X_{20}$  polyhedra. These clathrates have a number of important differences with respect to fullerites (see Table I). From these, we can underline the nature of the cage-atoms. Even if calculations predict that carbon clathrates are energetically favourable, up to now only Si, Ge or Sn clathrates have been synthesized. The synthesis process of group-14 clathrates needs the participation of template atoms for the cage formation. This results in the endohedral intercalation of these atoms in nano-cage structures that constitute the other major difference with respect to fullerites. Nevertheless, in the case of the type-II structure it has been possible to practically empty the cage structure [for a discussion see Ref. 24], giving rise to a new silicon semiconductor polytype with a gap of 1.9 eV.<sup>25</sup> The intercalated atoms include donor (alkali or alkali earth) and acceptor (I, Te) atoms, making of intercalated clathrates a totally degenerated silicon  $\text{sp}^3$  structure, *i.e.*, metallic silicon.

The study of the high-pressure properties of group-14 clathrates is motivated by both fundamental and applied reasons. In fact, as we will later see, a major property of group-14 clathrates is the high cohesive character, which translates into elevated values of the bulk modulus. The

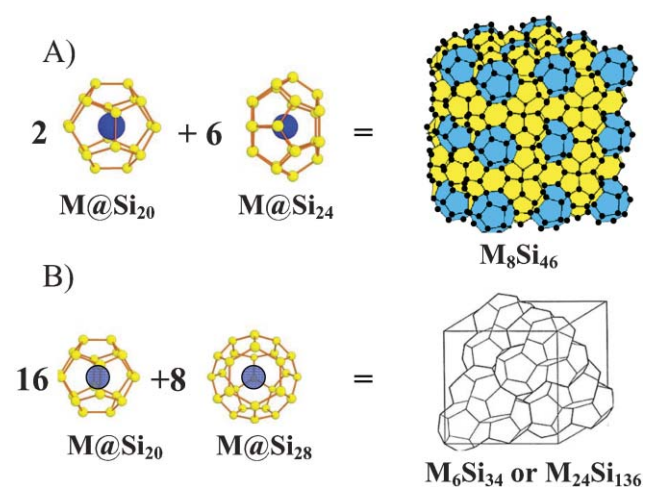


**Fig. 9** Structure of type-I (A) and type-II (B) silicon clathrates. The structures can be viewed as the combination of the  $\text{M@X}_{20}$  endofullerene with respectively  $\text{M@X}_{24}$  in type-I or  $\text{M@X}_{28}$  in type-II. All resulting structures are cubic and constituted by face-sharing association of the polyhedra. Type-I space group is  $\text{Pm}\bar{3}\text{n}$  with typical cell parameters of 10.19 Å ( $\text{Na}_8\text{Si}_{46}$ ) and  $\text{Fd}\bar{3}\text{m}$  for type-II and cell parameter 14.62 Å ( $\text{Si}_{136}$ ).

mechanical properties, in particular for the hypothetical carbon clathrates, are extremely interesting in this regard. A further feature of these structures is their extreme high-pressure stability that can be attributed to the particular interaction between guest atoms and the host lattice. From this point of view, the application of pressure constitutes an extremely valuable tool to explore the atom–cage interaction, which is of fundamental importance for the understanding of most of the clathrate properties giving rise to potential applications. From all these properties, superconductivity is probably one of the most attractive. In fact, convenient intercalation of Si or Ge clathrates gives rise to superconductivity with critical temperatures not exceeding 8.5 K. In the case of carbon clathrates, calculations predict much higher values. As a major interest of high-pressure in the study of clathrates, we have to underline that the combined extreme conditions of pressure and temperature have already allowed the synthesis of an important number of group-14 clathrates, in particular the best superconductors, and appears as a route of choice for the elaboration of other new clathrate forms.

Contrary to the case of fullerenes, which have been identified in meteorites and are expected to be present in interstellar space, no natural forms of group 14 clathrates have been identified up to now. We should nevertheless note that a potential identification of a carbon clathrate material may have been made in a natural sample, namely a rock impacted by a meteorite.<sup>26</sup> In good agreement with calculations on carbon clathrates hardness, the sample made of pure carbon was resistant to diamond polishing. X-ray diffraction showed a cubic structure with a large cell parameter of 14.697 Å, perhaps produced during the high-pressure, high-temperature conditions achieved during shock.

The first syntheses of germanium and silicon based clathrates by C. Cros, M. Pouchard *et al.* in 1965 were performed at low pressure. They were based on the decomposition under vacuum or argon of alkaline silicides ( $\text{NaSi}$ ,  $\text{KSi}$ ,  $\text{RbSi}$  and  $\text{CsSi}$ ). Clathrates can be synthesized at high-pressures, a route that appears as particularly advantageous in the synthesis of superconductive clathrates. The first high-pressure synthesis of a group 14 clathrate was realized in 2000 by the group of S. Yamanaka,<sup>27</sup> and concerned the type-I  $\text{Ba}_8\text{Si}_{46}$  clathrate. A stoichiometric mixture of  $\text{BaSi}_2$  and Si treated at 3 GPa, 800 °C for one hour allowed the elaboration of a close to pure sample. Since then, high-pressure synthesis has shown to be successful in different cases for the introduction of electronegative guest atoms (I, Se) or the elaboration of modifications of the type-I structures for instance type-III clathrates. The high-pressure synthesis and properties of group 14 clathrates, including superconductivity properties have been recently reviewed<sup>24</sup> and we refer readers to the references therein for further discussion.

As for fullerenes, the good choice of guest atoms in clathrates can give rise to superconductivity. Silicon clathrates were in fact the first known case of group 14  $\text{sp}^3$  superconductivity before the observation of superconductivity in high-pressure synthesized boron doped diamond. The mechanisms of superconductivity in clathrates appear to be different from the ones of the fullerites case, even if some aspects such as

the weight of electron–phonon coupling in the larger cages of the structure are still debated.

The first high-pressure structural study of the empty clathrate,  $\text{Si}_{136}$ <sup>28</sup> showed that the compressibility of the clathrate structure is only slightly lower than the one of the diamond case. This appears as a general aspect of group 14 clathrates that is just slightly modified by intercalation of different atomic species in the cage voids. Calculations on hypothetical carbon clathrate structures showed that their bulk modulus should be higher than cubic BN, the second hardest material after diamond. Predictions of the mechanical properties of such hypothetical carbon clathrates under strain, show that they should sustain limiting values comparable to diamond.

In spite of the fact that empty clathrates can be considered as expanded organized forms of the diamond structure, their stability under pressure is practically equivalent to the diamond one. X-ray diffraction studies show that the empty clathrate  $\text{Si}_{136}$ , transforms towards the silicon  $\beta$ -tin phase at about 11.5 GPa, *i.e.*, the same transition pressure as silicon diamond and the same high-pressure phase (Fig. 10). The clathrate stability can be extraordinarily modified through intercalation, with record stability limits obtained in the case of iodine intercalation (Fig. 10), that multiplies the stability

domain of the clathrate structure by a factor  $\sim 4$ ! The pressure stability of the clathrate phase in the different intercalated systems is mainly ruled by two factors: the size of the guest atoms and the hybridization between the host and the guest structure. Depending on these factors two different scenarios have been observed. The first one shared by Na intercalation and by the empty clathrate case, is the first order transformation of the structure towards the “normal” phase diagram of silicon. In the second case, observed in Ba, Ba–Sr, K, Rb, I intercalation, *i.e.*, with much larger atoms, the first order transformation is frustrated by the steric effect of intercalation. In that cases the clathrate structure is preserved up to pressures that can go beyond 40 GPa in some cases, ending by a pressure induced amorphization. The nature of the amorphous phase has not been yet elucidated, in particular whether or not a cage-like structure is preserved.

At pressures above the empty clathrate stability (11.5 GPa) but well below that of amorphization, a unique phase type of transition takes place. This transition corresponds to a homothetic volume collapse of the cubic structure associated with the appearance of some form of disorder. The pressure at which this homothetic volume collapse takes place can vary from  $13 \pm 2$  GPa in the case of  $\text{Ba}_8\text{Si}_{46}$  up to  $35 \pm 2$  GPa for  $\text{I}_8\text{Si}_{46-2.2}$ . The driving force of this isostructural transition is presently being studied considering several hypotheses such as electronic topological transition or incoherent hybridization instabilities. We develop here in more detail this last explanation. The homothetic constraint renders the cubic structures the only good candidates for such isostructural transitions. But as the atomic structure is not varied, the only way to modify the properties of the crystal in order to allow for a volume collapse is “to modify the atoms”. And this is in fact what has been proposed for the few cases where pressure induced isostructural volume collapse of cubic structures have been observed (Sm chalcogenides, Ce). This original idea was in fact first proposed by nuclear physicist E. Fermi in the case of Cs, in which pressure gives rise to an inversion between the s and d atomic orbitals of the atom. Finally, for this particular case, recent work has evidenced the non-isostructural character of the transition. The structure of the  $\text{M}_8\text{Si}_{46}$  type-I silicon clathrate can be viewed as the arrangement of  $\text{M}@\text{Si}_{20}$  and  $\text{M}@\text{Si}_{24}$  “superatoms”. The application of pressure modifies the size of the nano-cages. This opens the way for the existence of a critical size value at which the nature of the “super-atom” can be varied due to a modification of the hybridization between the guest atom and the host cage. This hybridization change inside the “super-atom” can break the symmetry of the molecule, for instance through the displacement of the guest atom from the centre of one of the cages. A displacement taking place incoherently in the cages of the crystal will generate a form of disorder that could be responsible of the experimental observations. In particular, from their study of  $\text{K}_8\text{Si}_{46}$ , Tse *et al.*<sup>29</sup> suggested that K atoms engaged in the Si cages play a crucial role for the phase transition; K atoms should be displaced under pressure from the center of  $\text{Si}_{24}$  cages causing a sudden disappearance of the phonon dispersion associated with the K vibration. In addition to the volume collapse and amorphization, other slight modifications of hybridization or in the dynamical properties

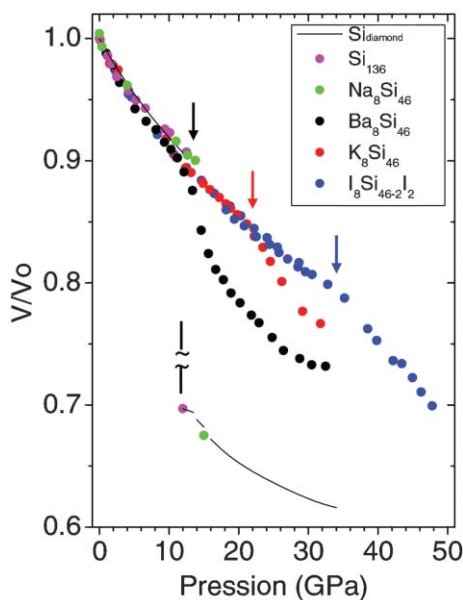


**Fig. 10** Compressibility and stability of silicon clathrates. The graph shows the pressure evolution of the relative volume of different silicon clathrates as compared with the diamond structure (line). Intercalation in silicon clathrates allows maintaining tetrahedral coordinated silicon up to pressures more than 4 times higher than in silicon diamond. The three coloured arrows point to the isostructural homothetic volume collapse transition (see text for details) of the (Ba, K or I) intercalated clathrates. The empty clathrate ( $\text{Si}_{136}$ ) and the Na intercalated clathrate follow a first order phase transformation merging with the silicon high-pressure phase diagram. The inner broken line is included to underline that, as clathrate are expanded forms of silicon, the relative volume after the phase transformation was renormalized to the one of silicon for the last point of  $\text{Si}_{136}$  and  $\text{Na}_8\text{Si}_{46}$ .

have been observed, in some cases at pressures below 10 GPa. The exact nature of such modifications are still under debate.

The Si clathrate stability is incomparably superior to that of clathrate hydrates (also called gas hydrates) that has not been found to exceed 1.6 GPa independently of the guest atom or molecule. This is clearly due to the high cohesive energy of the covalent tetrahedral  $sp^3$  bond. This remarkable clathrate stability allows the production of tetrahedral silicon with a low interatomic Si–Si distance of 2.15 Å which opens opportunities for chemical processes not yet explored. The minimum tetrahedral Si–Si interatomic distance attainable in clathrates could be even lower. In fact, the exact nature of the high-pressure amorphous phase of the silicon clathrates remains to be elucidated; in particular whether or not the amorphous phase is based on an arrangement of nano-cages.

#### 4. Nanotubes

We turn now to the last system that we examine in this review. Since their discovery in 1991 by Iijima carbon nanotubes have become one of the nanomaterials offering the highest potential for applications. In particular, functionalization through molecular binding or by intercalation or their potential use in electronic devices is extensively investigated. Nanotubes also present exceptional mechanical properties such as a Young's modulus of the order of TPa and an extreme resilience.<sup>30</sup> The main obstacle for the development of applications originates from the inhomogeneity of samples and the present impossibility of chemical or physical separation in homogeneous constituents. This fact, added to the strong interaction with pressure transmitting media, as was discussed in the introduction, constitute the major difficulties in high-pressure investigation of carbon nanotubes. As a consequence, even the clearest conclusions from *ab initio* calculations or other robust models are difficult to corroborate *via* experiments, making our understanding of the high-pressure behaviour of carbon nanotubes very incomplete.

Carbon nanotubes can be seen as a portion of a graphene plane (a single graphite plane) that has been cut and rolled to form a tube. Their dimensions,  $\sim$  nm in diameter and  $\sim$   $\mu$ m in length, make nanotubes prototypes for 1-dimensional crystalline systems. Depending on the growth process, single (SWNT) or multiple (MWNT) wall nanotubes can be obtained (Fig. 2). SWNT usually arrange in bundles of several tens of tubes in a hexagonal lattice (see Fig. 2). MWNT are concentric arrangements of up to several tens of tubes with inter-tube distances corresponding to the interlayer graphite distance, 3.41 Å. This is approximately the expected distance between typical SWNT in a bundle, but real samples can slightly differ from these expectations due for instance to a tube diameter distribution. The relative orientation of the rolling direction of the graphene plane with respect to the in-plane crystallographic axis of graphite, determines the chirality vector of a SWNT. All SWNT samples synthesized up to now present a diameter distribution and a chirality distribution. The 1-D character of the nanotubes gives rise to peaks in the electronic density of states named van Hove singularities, as shown in Fig. 1, which can lead to different resonant phenomena. Chirality determines the details of the electronic structure and for the same

tube diameter both semiconductor and metallic tubes are present in any particular sample due to the different chiralities present. For a review of the most significant properties of carbon nanotubes see for instance Ref. 31.

Carbon nanotubes are synthesized by different methods<sup>32</sup> including arc-discharge, laser ablation, chemical vapour deposition or high-pressure CO conversion (HiPCO). Hydrothermal synthesis of multiwall nanotubes has been also employed using polyethylene–water mixtures in the presence of nickel at 700–800 °C under 60–100 MPa pressure. This synthesis method gives rise to tubes that are shown to contain an encapsulated multiphase aqueous fluid, thus offering an attractive test platform for unique *in situ* nanofluidic experiments in the vacuum of a transmission electron microscope. Nevertheless, presently high-pressure synthesis of nanotubes is a minor synthesis method and we will not further develop it.

The conceptual simplicity and the originality of SWNT have probably motivated the concentration of high-pressure work with respect to MWNT and also our choice in this tutorial review. SWNT are expected to undergo through pressure application strong geometrical changes, nevertheless preserving their nanostructured character. In addition carbon nanotubes constitute already the building blocks of nano-mechanical devices, such as pressure sensors or resonators. All this has stimulated an important number of experimental and theoretical works concerning the high-pressure behaviour of SWNT. Nevertheless, comparison between experiments and calculations as well as between different experiments is not always easy. We detail this in the following paragraph.

Depending on the synthesis method, details of the synthesis protocol and on the purification techniques, carbon SWNT samples can be extremely different. Between the main parameters differentiating one sample from another, one can cite purity, tube size distribution, tube length, number of tubes on bundles, bundle crystallinity, or whether the tubes remain closed or have been opened. All these parameters can have an influence on the high-pressure properties of nanotubes and were not always considered in the first experimental articles on the high-pressure evolution of nanotubes. Independently of the synthesis method, we have also a chirality distribution in the sample, which has consequences on the mechanical properties and has only started to be investigated.

Up to now, the most used technique for the study of the high-pressure evolution of C-SWNT is Raman spectroscopy. Thanks to the presence of the van Hove singularities the Raman signal of C-SWNT is resonant, meaning that for a given incidence laser wavelength, only those tubes that can absorb the incident light *via* inter-singularity transition will provide a Raman signal. In particular for a given tube size distribution an optical selectivity *via* this resonance process of metallic or semiconductor tubes is made possible. On one hand this allows for selectivity, but on the other, these selection rules should be continuously modified by pressure application, as pressure modifies the band structure of the tubes, a factor that has rarely considered in high-pressure studies. High-pressure Raman spectroscopy experiments were reviewed in 2003<sup>33</sup> and the understanding of the high-pressure behaviour of carbon nanotubes is rapidly evolving but nevertheless remains incomplete.

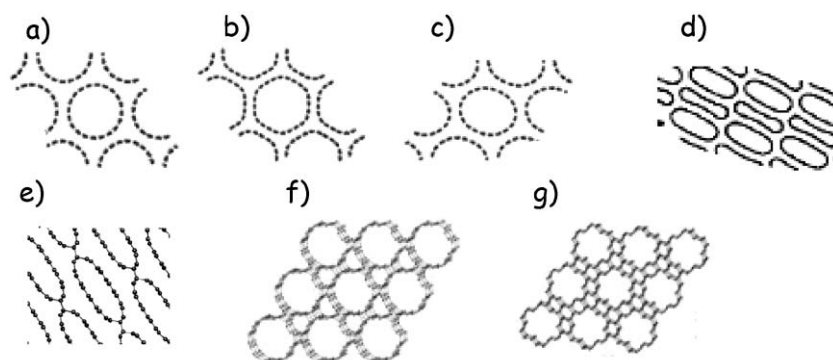


**Fig. 11** Some predicted pressure evolutions of bundled single wall carbon nanotubes. a) hexagonal structure at ambient conditions; b) hexagonal polygonization; c) ovalization; d) hybrid modification including racetrack type and peanut-like sections; e) 1-D polymerization of ovalized nanotubes; f and g) Two varieties of 2-D polymerization of non-deformed tubes.

The high-pressure evolution of nanotubes and the interpretation of experimental data is still debated. Nevertheless, based on experiments and calculations we can distinguish at least three main expected modifications in the high-pressure evolution of single wall nanotubes:

- The nanostructuration of the pressure transmitting medium.
- The modification of the nanotubes cross-section.
- The interlink between nanotubes.

The first parameters determining the pressure at which these transformations can take place are the nature of the pressure transmitting medium and the tube diameter. All mechanical properties of carbon nanotubes depend in first order on their tube diameter. Different theoretical studies agree in predicting a change of the section of the nanotubes that should evolve from circular to oval or hexagonal to peanut-like or even racetrack like (see Fig. 11). They predict a dependence of the critical pressure for this transition of the type  $P_c \sim 1/d^3$  for individual nanotubes, with  $d$ , the tube diameter. As an indication, for tubes diameter, ranging from 0.7 to 1.5 nm, the cross-section modification is expected to be found between 1 GPa for larger tubes and 12 GPa for the smaller ones. The effect of bundling on this transformation pressure is not clear as screening effects due to the presence of other tubes or diameter inhomogeneities can have reversed effects. On the other hand, one can expect this phase transformation to be governed by the instability of the bigger tubes which will create a non homogeneous strain field facilitating the collapse of smaller ones. To complicate this, nanostructuration of the pressure transmitting medium can take place at similar pressure regimes. The mechanical instability involving the modification of the tube cross-section is predicted to be of reversible nature, but with further pressure application, modifications including covalent bonding between tubes have been also predicted (Fig. 11). Irreversible inter-tube covalent binding has been also observed through electronic bombardment of bundles of SWNT, leading to an improvement of the mechanical properties of the bundle.

As an illustration of the contrasting differences on the high-pressure behaviour of SWNT depending on samples and experimental conditions, we will consider here two extreme cases:

a) Purified arc-discharge synthesized and open C-SWNT highly crystallized bundles of approximately 50 tubes pressurized with argon as pressure transmitting medium.<sup>34</sup> In this case argon is the pressure transmitting medium and also fills the inner channel of the nanotubes composing the bundles.

b) As-prepared HiPco-synthesized closed C-SWNT individualized (debundled) and isolated by a 50 nm layer of surfactant (sodium cholate), the whole deposited on glass microfibers and pressurized with 4 : 1 methanol : ethanol mixture<sup>35</sup>

Fig. 12 illustrates the structural differences between the two types of systems study, of which gave rise to much contrasted results. In a) the nanotubes could sustain pressures as high as 40 GPa without showing any characteristic sign of phase transformation. After pressure recovery from 15 GPa, very small modifications of the Raman signal were visible. The radial breathing modes (RBM) which are detected at low energies, disappeared at pressures of 4 and 10 GPa respectively for semiconductor and metallic tubes of approximately the same size of 1.4 nm. This attenuation was attributed to resonance loss. Our example in a) constitutes also the highest pressure study of SWNT under quasi-hydrostatic pressure<sup>34</sup> and revealed that nanotubes do not reverse completely after a pressure cycle going up to 40 GPa. In b) modifications in the

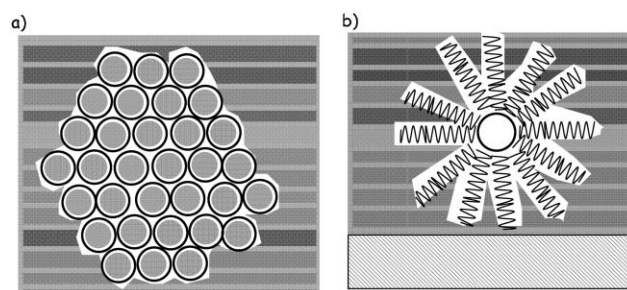


**Fig. 12** Scheme of the experimental configuration for two single-wall carbon nanotube systems as explained in the text. a) Nanotube bundles of open SWNT immersed in argon as pressure transmitting medium with argon penetrating the inner channel of the nanotubes. b) Closed SWNT individualized and isolated by a 50 nm layer of surfactant. The whole deposited on glass microfibers and pressurized with 4 : 1 methanol : ethanol mixture.

pressure evolution of the Raman shift of the nanotubes tangential modes were clearly visible at 4 GPa. This type of change has been tentatively attributed to adsorption like molecular ordering of the pressure transmitting medium around the nanotubes. The RBM and the high energy transverse modes disappeared simultaneously at  $P_c$  of 3.5 and 10 GPa for tubes of 1.2–1.3 nm and 0.8–0.9 nm respectively and was attributed to the collapse of nanotubes, scaling well with the predicted phase transformation related to the change of the nanotubes cross-section,  $P_c \sim 1/d^3$  already mentioned.

Under high-pressure and high-temperature conditions, carbon nanotubes are an expensive alternative for diamond synthesis, and several works have demonstrated this possibility. What is really more interesting is the formation of other carbon phases from carbon nanotubes. Polymerized-SWNT were synthesized by Khabashesku *et al.*<sup>36</sup> by high pressure and high temperature treatment as well as nano- and microcrystalline diamond-like (cubic and hexagonal) and nanographite. A. Popov *et al.*<sup>37</sup> obtained also polymerized-SWNT by applying a shear deformation under load at a pressure of 24 GPa. The obtained sample exhibited mechanical properties comparable or exceeding the ones of cubic boron nitride, the hardest material after diamond. Z. Wang *et al.*<sup>38</sup> report the formation of a nano-sized  $sp^3$ -rich hexagonal polymorph of carbon from the cold compression of SWCNT bundles without pressure transmitting medium. The new phase is observed at  $\sim 75$  GPa and is preserved after pressure release presenting mechanical properties comparable to the ones of nano-diamond which, as we mentioned, are superior to those of bulk diamond.

Nanotubes can also be used as “crucibles” for high-pressure chemistry at the nanoscale. We can here consider two different scenarios. The nanotubes used as nano-anvils or the nanotubes as nano-pistons. In the first one the compression of the nanotubes by the pressure transmitting medium act on the systems intercalated inside the nanotubes. In the second one the penetration of the pressure transmitting medium inside the tube pressurizes the encapsulated system. Many different substances can be introduced in the nanotubes, including hydrogen, halogens, metals or even molecules as fullerenes. We can cite the recent work of S. Kawasaki *et al.*<sup>39</sup> where the nanotube cavity was used to induce the 1-D chain polymerization of  $C_{60}$  molecules inserted inside the nanotubes (a system known as a “peapod” for obvious reasons).

Also, electron irradiation of multiwall nanotubes filled with different materials can lead to similar results. In fact, irradiation defect formation generates a stress that is transmitted to the system filling the tube and can generate pressures as high as 40 GPa, giving rise to nano-extrusion phenomena eventually generating phase transformations.<sup>40</sup>

#### 4. Conclusions

We have covered non exhaustively the high-pressure behaviour of the main homogeneous nanomaterials families. We have chosen to cover those systems for which a considerable amount of literature already exists. Consequently a certain number of systems as multi-wall carbon nanotubes, carbon nano-onions, nanowires or other types of non-carbon

nanotubes have not been discussed. We have focused our discussion on the phase-diagrams, size effects and the importance of intercalation or other interactions with the pressure transmitting medium when present. The presented results on nanocrystals, nano-cage based materials and carbon nanotubes demonstrate that high-pressure or its combination with high-temperature is a very powerful means to modify nanostructured materials, study interactions at the nanoscale and elaborate new nanomaterials.

We wanted to show that the study of nanomaterials under high pressure and high temperature conditions offers new paths both for the investigation of fundamental phenomena and for the elaboration of new materials with new or improved properties. Three different mechanisms participate in these modifications: transformation of the nano-object itself, nano-assembling and the modification of the interaction of the nano-object with its environment. In some cases these transformations preserve nanostructuring, allowing all the benefits related with all the technological potentials of the nanoworld to be maintained.

In particular, we have seen that the interaction of the pressure transmitting medium with the nanosystems is favoured by their very nature, *i.e.*, the importance of surface atoms in nanostructuring. Taking into account these interactions or using them to control chemical processes, constitutes one of the important challenges of high-pressure investigations of nanomaterials.

The future developments of high-pressure nanomaterials investigations are difficult to assess but many emerging subjects start to trace new routes. The investigation of individual or individualized nano-objects appears as one of these important routes. Use of atomic microscopic techniques or strong resonant phenomena for instance allow for the investigations of pressure effects on individual objects. This approach allows going beyond the limitations due to sample inhomogeneities as size or shape distributions, for instance. Then the study of the pressure behaviour of a potentially well characterized nano-object and an ideal confrontation with model calculations will be possible. As well, such an approach allows us to study separately the pressure effect on the nano-object itself from the interaction with other nano-objects, a necessary step for nano-architectural approaches

Another rapidly growing field is controlled nano-intercalation which provides the nanosystem with donor–acceptor atoms or spacer partners. High-pressure can play an important role in different ways. Firstly, combining high-pressure and high-temperature conditions with chemical control allows the exploration of new bonding schemes in intercalated systems with potential for generating novel families of nanomaterials. Secondly, intercalation offers a new path for the study of the high-pressure properties of new low-dimensional systems. This is for instance the case of the endohedral filling of carbon nanotubes which allows new 1-D nanoconfined systems to be obtained. The host nanostructure properly combined with the pressure transmitting medium allows for the development of nanopresses and nanopistons and access to totally unexplored scientific domains. Nanoscience and consequently the high-pressure study of nanomaterials is an appealing, young and highly expanding research area, with space both for applied

and fundamental investigations. It will undoubtedly open lines and roads of study beyond present ideas and concepts.

## Acknowledgements

I would like to thank P. F. McMillan for his careful reading of the manuscript and his useful remarks as well as M. Pouchard, from the French Academy of Science for his remarks concerning the clathrate section.

## References

- 1 V. G. Gryaznov, I. A. Polonsky, A. E. Romanov and L. I. Trusov, *Phys. Rev. B: Condens. Matter*, 1991, **44**, 42.
- 2 C.-C. Chen, A. B. Herhold, C. S. Johnson and A. P. Alivisatos, *Science*, 1997, **276**, 398.
- 3 D. Zaziski, S. Prilliman, E. C. Scher, M. Casula, J. Wickham, X. M. Clark and A. P. Alivisatos, *Nano Lett.*, 2004, **4**, 943.
- 4 C. T. Dameron, R. N. Reese, R. K. Mehra, A. R. Kortan, P. J. Carroll, M. L. Steigerwald, L. E. Brus and D. R. Winge, *Nature*, 1989, **338**, 596.
- 5 S. H. Tolbert and A. P. Alivisatos, *J. Chem. Phys.*, 1995, **102**, 4642.
- 6 J. Z. Jinag, *J. Mater. Sci.*, 2004, **39**, 5103.
- 7 B. Palosz, S. Stel'makh, E. Grzanka, S. Gierlotka, R. Pielaszek, U. Bismayer, S. Werner and W. Palosz, *J. Phys.: Condens. Matter*, 2004, **16**, S353.
- 8 J. Y. Ratty and G. Galli, *Nat. Mater.*, 2003, **2**, 792.
- 9 S. M. Clark, S. G. Prilliman, C. K. Erdonmez and A. P. Alivisatos, *Nanotechnology*, 2006, **16**, 2813.
- 10 A. P. Alivisatos, *J. Phys. Chem.*, 1996, **100**, 13226.
- 11 K. Jacobs, D. Zaziski, E. C. Scher, A. B. Herhold and A. P. Alivisatos, *Science*, 2001, **293**, 1803.
- 12 F. Decremps, J. Pellicer-Porres, F. Datchi, J. P. Itié, A. Polian, F. Baudelet and J. Z. Jiang, *Appl. Phys. Lett.*, 2002, **81**, 4820.
- 13 S. H. Tolbert, A. B. Herhold, L. E. Brus and A. P. Alivisatos, *Phys. Rev. Lett.*, 1996, **76**, 4384.
- 14 S. K. Deb, M. Wilding, M. Somayazulu and P. F. McMillan, *Nature*, 2001, **414**, 528.
- 15 V. Swamy, A. Kuznetsov, L. S. Dubrovinsky, P. F. McMillan, V. B. Prakapenka, G. Shen and B. C. Muddle, *Phys. Rev. Lett.*, 2006, **96**, 135702.
- 16 T. Irifune, A. Kurio, S. Sakamoto, T. Inoue and H. Sumiya, *Nature*, 2003, **421**, 599.
- 17 J.-Y. Raty, G. Galli, C. Bostedt, T. W. van Buuren and J. Terminello Louis, *Phys. Rev. Lett.*, 2003, **90**, 037401.
- 18 B. Sundqvist, *Adv. Phys.*, 1998, **48**, 1.
- 19 R. Moret, *Acta Crystallogr.*, 2005, **A61**, 62.
- 20 M. V. Korobov, V. M. Senyavin, A. G. Bogachev, E. B. Stukalin, V. A. Davydov, L. S. Kashevarova, A. V. Rakhmanina, V. Agafonov and A. Szwarc, *Chem. Phys. Lett.*, 2003, **381**, 410.
- 21 L. Marques, M. Mezouar, J.-L. Hodeau, M. Núñez-Regueiro, N. R. Serebryanaya, V. A. Ivdenko, V. D. Blank and G. A. Dubitsky, *Science*, 1999, **283**, 1720.
- 22 S. Yamanaka, A. Kubo, K. Inumaru, K. Komaguchi, N. S. Kini, T. Inoue and T. Irifune, *Phys. Rev. Lett.*, 2005, **96**, 076602.
- 23 S.-N. Luo, O. Tschauner, T. E. Tierney, IV, D. C. Swift, S. J. Chipera and P. D. Asimow, *J. Chem. Phys.*, 2005, **123**, 024703.
- 24 A. San Miguel and P. Toulemonde, *High Pressure Res.*, 2005, **25**, 159.
- 25 J. Gryko, P. F. McMillan, R. F. Marzke, G. K. Ramachandran, D. Patton, S. K. Deb and O. F. Sankey, *Phys. Rev. B: Condens. Matter Mater. Phys.*, 2000, **62**, 7707.
- 26 A. El Goresy, L. S. Dubrovinsky, Ph. Gillet, S. Mostefaoui, G. Graup, M. Drakopoulos, A. S. Simionovici, V. Swamy and V. L. Masaitis, *C. R. Geosci.*, 2003, **335**, 889.
- 27 S. Yamanaka, E. Enishi, H. Fukuoka and M. Yasukawa, *Inorg. Chem.*, 2000, **39**, 56.
- 28 A. San-Miguel, P. Keghelian, X. Blase, P. Mélinon, A. Perez, A. Polian, J.-P. Itié, E. Reny, C. Cros and M. Puchard, *Phys. Rev. Lett.*, 1999, **83**, 5290.
- 29 J. S. Tse, S. Desgreniers, Z.-qiang Li, M. R. Ferguson and Y. Kawazoe, *Phys. Rev. Lett.*, 2002, **89**, 195507.
- 30 See for a review: D. Qian, G. J. Wagner, W. K. Liu, M.-F. Yu and R. S. Ruoff, *Appl. Mechanics Rev.*, 2002, **55**, 495.
- 31 S. Reich, Ch. Thomsen and J. Maultzsch, in *Carbon Nanotubes: Basic Concepts and Physical Properties*, Wiley-VCH, Berlin, 2004.
- 32 See for a recent review: C. N. R. Rao and A. Govindaraj, in *Nanomaterial synthesis: Nanotubes and nanowires*, Royal Society of Chemistry, Cambridge, UK, 2005.
- 33 I. Loa, *J. Raman Spectrosc.*, 2003, **34**, 611.
- 34 A. Merlen, N. Bendiab, P. Toulemonde, A. Aouizerat, A. San Miguel, J. L. Sauvajol, G. Montagnac, H. Cardon and P. Petit, *Phys. Rev. B: Condens. Matter Mater. Phys.*, 2005, **72**, 035409.
- 35 S. Lebedkin, K. Arnold, O. Kiowski, F. Hennrich and M. M. Kappes, *Phys. Rev. B: Condens. Matter Mater. Phys.*, 2006, **73**, 094109.
- 36 V. N. Khabashesku, Z. Gu, B. Brinson, J. L. Zimmerman, J. L. Margrave, V. A. Davydov, L. S. Kashevarova and A. V. Rakhmanina, *J. Phys. Chem. B*, 2002, **106**, 11155.
- 37 M. Popov, M. Kyotani, R. J. Nemanich and Y. Koga, *Phys. Rev. B: Condens. Matter Mater. Phys.*, 2002, **65**, 033408.
- 38 Z. Wang, Y. Zhao, K. Tait, X. Liao, D. Schiferl, C. Zha, R. T. Downs, J. Qian, Y. Zhu and T. Shen, *Proc. Natl. Acad. Sci. USA*, 2004, **101**, 13699.
- 39 S. Kawasaki, T. Hara, T. Yokomae, F. Okino, H. Touhara, H. Kataura, T. Watanuki and Y. Ohishi, *Chem. Phys. Lett.*, 2006, **418**, 260.
- 40 L. Sun, F. Banhart, A. V. Krashennnikov, J. A. Rodríguez-Manzo, M. Terrones and P. M. Ajayan, *Science*, 2006, **312**, 1199.
- 41 V. D. Blank, S. G. Buga, G. A. Dubitsky, N. R. Serebryanaya, N. Yu. Popov and B. Sundqvist, *Carbon*, 1998, **36**, 319.
- 42 A. V. Talyzin, L. S. Dubrovinsky, T. Le Bihan and U. Jansson, *J. Chem. Phys.*, 2002, **116**, 2166.
- 43 M. Núñez-Regueiro, L. Marques and J.-L. Hodeau, *The Physics of fullerene-based and fullerene-related materials*, ed. W. Andreoni, Kluwer Academic Dordrecht and Boston, 2000.
- 44 K. Jacobs, J. Wickham and A. P. Alivisatos, *J. Phys. Chem. B*, 2002, **106**, 3759.